J Vet Sci. 2023 May;24(3):e23
https://doi.org/10.4142/jvs.22083
pISSN 1229-845X·eISSN 1976-555X

Journal of Veterinary Science

Original Article
Pharmacology

Check for updates

Therapeutic effects of paeoniflorin on irritable bowel syndrome in rats

Lei Wang [1,2,†], **Jinyan Lei** [2,3,†], **Zeyu Zhao** [4], **Jianwei Jia** [2,3,*], **Li Wang** [1,5,*]

[1]Department of Pharmacy, Tianjin Second People's Hospital, Tianjin 300192, China
[2]Tianjin Institute of Hepatology, Tianjin 300192, China
[3]Department of Integrated Chinese and Western Medicine, Tianjin Second People's Hospital, Tianjin 300192, China
[4]School of Integrative Medicine, Tianjin University of Traditional Chinese Medicine, Tianjin 301600, China
[5]Academy of Medical Engineering and Transnational Medicine, Tianjin University, Tianjin 300072, China

OPEN ACCESS

Received: Mar 25, 2022
Revised: Oct 9, 2022
Accepted: Oct 14, 2022
Published online: Feb 17, 2023

***Corresponding authors:**
Jianwei Jia
Department of Pharmacy, Tianjin Second People's Hospital and Tianjin Institute of Hepatology, No. 75, Sudi Road, Nankai District, Tianjin 300192, China.
Email: jiajwtsph@peak-edu.cn
https://orcid.org/0000-0002-6510-4201

Li Wang
Department of Pharmacy, Tianjin Second People's Hospital and Academy of Medical Engineering and Transnational Medicine, Tianjin University, 92 Weijin Road, Nankai District, Tianjin 300072, China.
Email: wanglitsph@ymail.cn
https://orcid.org/0000-0001-5025-5536

[†]Lei Wang and Jinyan Lei contributed equally to this study.

ABSTRACT

Background: Irritable bowel syndrome (IBS) is a functional bowel disorder (FBD).
Objectives: To assess the therapeutic effects of paeoniflorin (PF) on IBS in rats.
Method: Sixty male Sprague–Dawley rats were randomly divided into normal, model, positive drug, low-dose PF, medium-dose PF and high-dose PF groups (n = 10). After gavage for 2 consecutive weeks, the effect of PF on abdominal pain symptoms was assessed based on the abdominal withdrawal reflex (AWR) score, fecal water content and pathological changes in colon tissues. D-lactate, interleukin-1β (IL-1β), transforming growth factor-β (TGF-β) and tumor necrosis factor-α (TNF-α) were detected by enzyme-linked immunosorbent assay, and phosphorylated nuclear factor kappa B (p-NF-κB) p65 was detected by Western blotting. The abundance and diversity changes of intestinal flora were explored using 16S ribosomal RNA sequencing.
Result: In PF groups, the mucosal morphology of colon tissues was intact, and the glands were arranged neatly and structured clearly, without obvious inflammatory cell infiltration. Compared with the model group, PF groups had significantly elevated pain threshold, and mRNA and protein levels of zonula occludens-1 (ZO-1) and occludin, decreased AWR score at 20 mmHg pressure, fecal water content, mRNA levels of IL-1β, TGF-β, and TNF-α, protein level of p-NF-κB p65 and level of serum D-lactate, and reduced levels of serum IL-1β, TGF-β, and TNF-α ($p < 0.05$, $p < 0.01$). PF groups had higher abundance of *Lactobacillus*, *Akkermansia*, *Alistipes*, and *Bacteroides*, but lower abundance of *Desulfovibrio*, *Parasutterella*, and *Enterococcus* than those of the model group.
Conclusions: PF exerts therapeutic effects on IBS in rats probably by regulating the intestinal flora, and then up-regulating the expressions of ZO-1 and occludin in colon tissue while down-regulating the levels of IL-1β, TGF-β, TNF-α, D-lactate and p-NF-κB p65.

Keywords: Colon; intestinal flora; sequence analysis, RNA; enzyme-linked immunosorbent assay; abdominal pain

INTRODUCTION

Irritable bowel syndrome (IBS) is a functional bowel disorder (FBD) primarily manifested as the alleviation or relief of abdominal pain and discomfort after defecation, accompanied by changes in defecation habits and stool properties. With persistent or intermittent symptoms,

ORCID iDs
Lei Wang
https://orcid.org/0000-0003-3458-7711
Jinyan Lei
https://orcid.org/0000-0002-5794-1907
Zeyu Zhao
https://orcid.org/0000-0002-2086-8160
Jianwei Jia
https://orcid.org/0000-0002-6510-4201
Li Wang
https://orcid.org/0000-0001-5025-5536

Author Contributions
Conceptualization: Wang L, Lei J, Wang L; Data curation: Wang L, Lei J, Zhao Z; Formal analysis: Zhao Z; Software: Jia J, Wang L; Writing - original draft: Wang L, Jia J, Wang L; Writing - review & editing: Wang L.

Conflict of Interest
The authors declare no conflicts of interest.

Funding
This study was financially supported by Tianjin Medical Key Construction Discipline Fund Project (No. 2021-492).

it is characterized by complex pathogenesis and influenced by several factors [1-3]. Repeated attacks of such symptoms affect the study, life and work of patients. Therefore, finding novel therapies for IBS is of great clinical significance.

Intestinal microorganism is a diverse ecosystem with numerous members in the entire gastrointestinal tract, and it has a systemic impact on human health. It is composed of four main types of bacteria, among which Gram-positive Firmicutes (including more than 180 kinds of Lactobacillus) and Actinomycetes (including *Bifidobacterium*), and Gram-negative Bacteroides (mainly *B. Fragilis*) and Proteobacteria (*Escherichia coli*, *Salmonella*, *Vibrio*, *Haemophilus*, *etc.*) are most abundant. The changes of intestinal flora in IBS pathophysiology have been well-documented, but its etiological role remains unclear [4,5]. The intestinal flora disturbance can affect human emotions and behaviors, and anxiety and depression are often concurrent with IBS in most cases [6]. Some patients with IBS have increased Firmicutes/Bacteroidetes ratio, which may be associated with depression and anxiety. In addition, different microbial compositions have been found in IBS patient-to-mouse fecal transplants, and the mice receiving IBS fecal transplants display different serum metabolomics characteristics, which are related to the enhanced gastrointestinal motility, intestinal barrier disorders and innate immune activation.

Tongxieyao Formula and Xiaoyao Powder are the most commonly used traditional Chinese medicine (TCM) compound prescriptions for IBS [7]. Radix Paeoniae Alba, as the main component in the above-mentioned prescriptions, can calm the liver and relieve pain, nourish blood for regulating menstruation, retain yin with astringent and stop sweating. According to TCM pharmacological studies, Radix Paeoniae Alba has immunoregulatory and anti-inflammatory activities, and its main active ingredient is total glucoside of paeony [8]. Until now, its specific mechanism of action on IBS remains elusive. As a monoterpenoid glycoside, paeoniflorin (PF) is one of the main active ingredients of Paeoniae Alba. PF can markedly relieve the pain induced by bee venom in mice, mitigate colitis in mice, and resist adjuvant arthritis in rats [9]. In this study, therefore, the therapeutic effect of PF on IBS was evaluated from the perspective of intestinal flora, and the regulatory effect of PF on the intestinal flora of IBS rats was investigated using 16S ribosomal RNA (rRNA) sequencing, aiming to clarify the mechanism for treating intestinal diseases.

MATERIALS AND METHODS

Laboratory animals

Male Sprague–Dawley (SD) rats weighing 200 ± 20 g were purchased from Beijing Huafukang Biotechnology Co., Ltd. (China; SCXK [Beijing] 2020-0004). They were adaptively fed for 1 week in a quiet environment with 55%–60% relative humidity, and had free access to adequate clean drinking water and food. This study has been approved by the animal ethics committee of Tianjin Second People's Hospital (approval No. 2021-SYDWLL-000038). During the experiment, the 3R principle was followed, and the animals were given humanitarian care.

Main drugs and apparatus

The main reagents used included PF (purity ≥ 99%, S31585) (Shanghai YuanYe Biotechnology Co., Ltd., China), rifaximin (R126176) (Shanghai Aladdin Bio-Chem Technology Co., Ltd., China), enzyme-linked immunosorbent assay (ELISA) kits of D-lactate (E02D0015), interleukin-1β (IL-1β; E02I0010), transforming growth factor-β (TGF-β; E02T0058), and tumor necrosis

factor-α (TNF-α; E02T0008) (Shanghai BlueGene Biotech Co., Ltd., China), nuclear factor kappa B (NF-κB) p65 antibody (10745-1-AP) (Proteintech, Japan), phosphorylated (p-)NF-κB p65 antibody (#3033) (CST, USA), zonula occludens-1 (ZO-1) antibody (61-7300) and occludin antibody (71-1500) (Thermo Fisher Scientific Co., Ltd., China), total RNA extraction kits (#DP419), complementary DNA (cDNA) reverse transcription kits (KR116-02) and SYBR amplification kits (#P205-02) (Tiangen Biotech [Beijing] Co., Ltd., China).

The main instruments included high-performance universal benchtop refrigerated centrifuge (Thermo Fisher Sorvall ST16R; Thermo Scientific, USA), multi-function microplate reader (Thermo Scientific), optical microscope (Nikon ECLIPSE TS100; Nikon Japan), and fluorescence quantitative polymerase chain reaction (PCR) system (Bio-Rad iQ5; Bio-Rad, USA).

IBS rat modeling

The number of required rats was calculated according to $n = (t_{0.05} \times S_d)^2/d^2$, where S_d is the variance of intergroup difference, d is the mean difference when the expected difference is significant, and $t_{0.05}$ is the t value at a certain df when a=0.05. Assuming n > 30 and t = 2, n was calculated as 9 based on $S_d = 3$ and d = 2. In other words, no less than 9 rats should be included in each group, so 10 rats in each group were finally selected in this study. A total of 60 male SD rats were randomly divided into normal, model, positive drug, low-dose PF, medium-dose PF and high-dose PF groups (n = 10). The IBS rat model was established except for the normal group.

The IBS rat model was established using 4% acetic acid enema combined with chronic psychological stress [10]. First, after fasting for 1 day, the rats were anesthetized with ether, and a 6F infant catheter coated with lubricant was inserted by 6 cm. For normal group and other groups, 1 mL of 0.9% sodium chloride solution and 4% acetic acid solution were injected, respectively. About 30 sec later, 1 mL of 0.9% sodium chloride solution was injected to wash away the remaining solution. Chronic psychological stresses included odor stimulation, humid environment, reversal of night and day, sound stimulation, electric shock, restraint, strong light and flashing light exposure, water and food deprivation, crowding, tail clamp, noise and cage tilt. One stress was randomly given in the morning and afternoon each for 14 days, and the same stress was not continuously used. The model establishment was considered successful if the fecal water content increased compared with that of the normal group.

Administration regimen

In the pre-experiment, the lethal dose of PF for rats was 300 mg/kg, so 1/10 of the lethal dose, i.e., 30 mg/kg, was selected for the high-dose group. Meanwhile, 2/3 of the high dose, i.e., 20 mg/kg, was used for the medium-dose group, and 1/2 of the medium dose, i.e., 10 mg/kg, was selected for the low-dose group. After modeling, normal and model groups were gavaged with 0.2 mL of normal saline every day, the positive drug group was gavaged with rifaximin at 150 mg/kg every day, and low-dose, medium-dose and high-dose PF groups were gavaged with PF at 10 mg/kg, 20 mg/kg and 30 mg/kg every day respectively for 2 consecutive weeks. The flowchart is exhibited in **Fig. 1**.

Visceral sensitivity measurement

Before the start of the experiment, the rats were deprived of food but not water overnight. At the beginning of the experiment, the rats were anesthetized with isoflurane, and a paraffin oil-lubricated pressure tube with a balloon was inserted into the deep anus and fixed at the root of the tail using adhesive tapes. The rats were confined to a transparent box. After they

https://doi.org/10.4142/jvs.22083

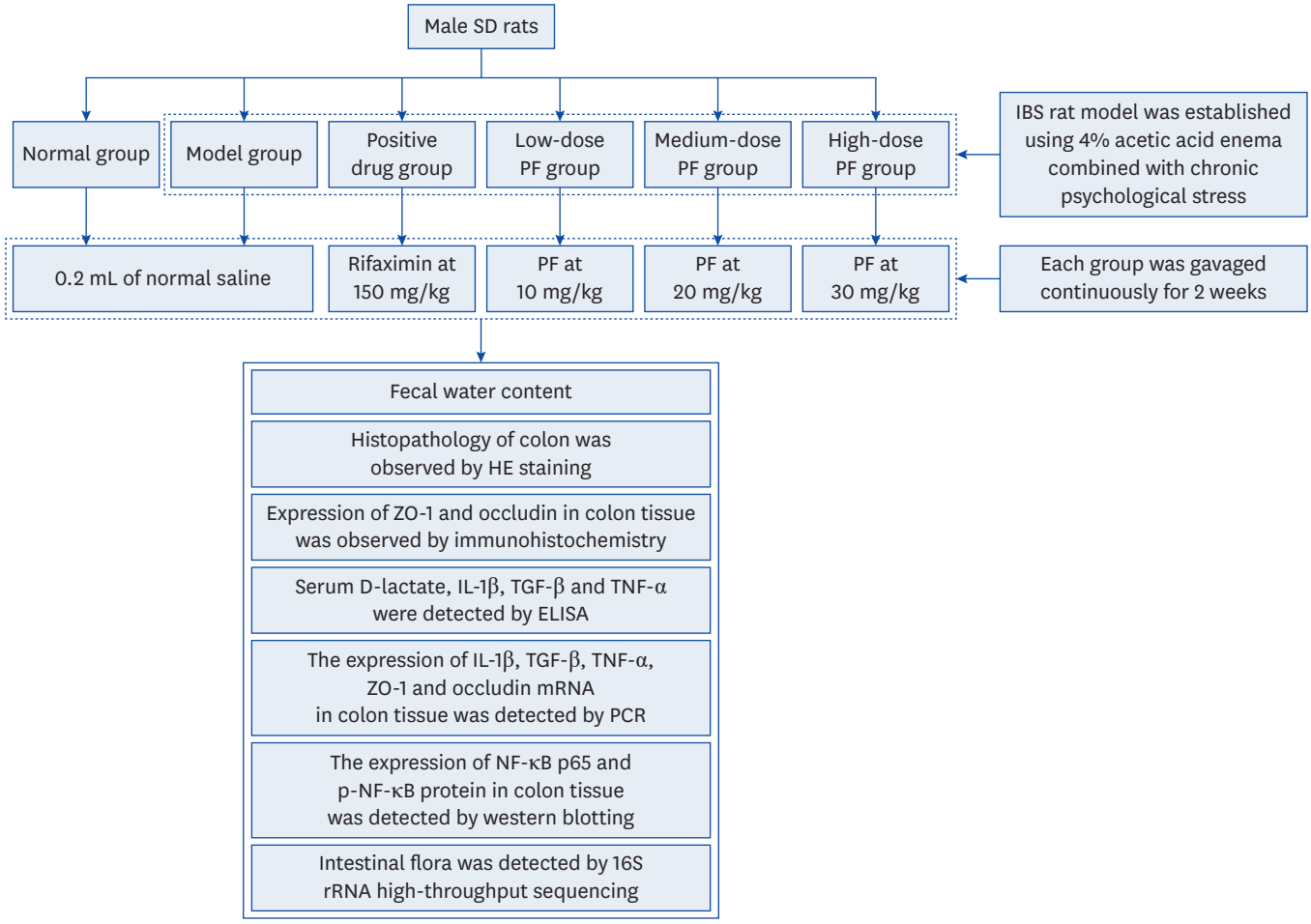

Fig. 1. Study flowchart.
SD, Sprague–Dawley; PF, paeoniflorin; IBS, irritable bowel syndrome; HE, hematoxylin-eosin; ZO-1, zonula occludens-1; IL-1β, interleukin-1β; TGF-β, transforming growth factor-β; TNF-α, tumor necrosis factor-α; ELISA, enzyme-linked immunosorbent assay; ZO-1, zonula occludens-1; mRNA, messenger RNA; PCR, polymerase chain reaction; NF-κB, nuclear factor kappa B; p-NF-κB, phosphorylated nuclear factor kappa B; rRNA, ribosomal RNA.

became awake and fully quiet, the balloon was inflated to simulate the intestinal sensitivity to mechanical stimulation, causing rectal distention to induce abdominal withdrawal reflex (AWR). The pressure was applied at 20, 40, 60 and 80 mmHg respectively for 20 sec every 4 min. The mean AWR score was given in 3 measurements at each pressure, and the scoring criteria were as follows: 0 point: no obvious changes, 1 point: mild anxiety such as head twisting, and no contraction of the abdomen-back muscle, 2 points: mild contraction of the abdomen-back muscle, and the abdomen does not lift off the ground, 3 points: moderate contraction of the abdomen-back muscle, and the abdomen lifts off the ground, 4 points: severe contraction of the abdomen-back muscle, bow-shaped abdominal bending, and the abdomen lifts off the ground. The pressure threshold when the AWR score was 3 points was used as the pain threshold [11].

Evaluation of effects of PF on fecal water content of rats with IBS

The rats were placed in metabolic cages for 24 h and given adequate food and water. The feces were collected and weighed as the wet weight, and then they were dried and weighed as the dry weight. Finally, the fecal water content was calculated as: (Wet Weight − Dry Weight)/Wet Weight.

https://doi.org/10.4142/jvs.22083

Evaluation of effects of PF on colon tissue pathology of rats with IBS by hematoxylin-eosin (HE) staining

After modeling and administration, the colon tissues were harvested, fixed with formalin solution, embedded in paraffin, and sliced into 3 μm-thick sections, followed by routine HE staining. The pathological changes in colon tissues were observed under an optical microscope.

Evaluation of effects of PF on ZO-1 and occludin expressions in colon tissues of rats with IBS by immunohistochemical staining

The paraffin sections of colon tissues were routinely deparaffinized and dehydrated, subjected to antigen retrieval, blocked, and incubated with primary antibodies (ZO-1 and occludin) at 4°C overnight and then with secondary antibodies, followed by color development with DAB and hematoxylin counterstaining. The sections were photographed under the microscope. The positive staining area was quantified using Image Pro Plus 6.0 (Media Cybernetics, Inc., USA), and the percentage of positive expression area was calculated.

Evaluation of effects of PF on serum D-lactate, IL-1β, TGF-β and TNF-α in rats with IBS by ELISA

After anesthesia, the rats were fixed, the abdominal cavity was opened, and blood was drawn from the abdominal aorta. After being left still at room temperature, the blood was centrifuged at 3,000 r/min and 4°C for 10 min. The supernatant was harvested by a pipette into a 2 mL EP tube and stored in a refrigerator at 80°C for later use. D-lactate, IL-1β, TGF-β, and TNF-α were detected according to the instructions of kits.

Evaluation of effects of PF on IL-1β, TGF-β, TNF-α, ZO-1, and occludin mRNA expressions in colon tissues of rats with IBS by PCR

After modeling and administration, total RNA was extracted from colon tissues, and reversely transcribed into cDNA using transcriptase, followed by PCR amplification, with cDNA as the template. The expressions of inflammation- and intestinal permeability-related genes IL-1β, TGF-β, TNF-α, ZO-1, and occludin in colon tissues were detected. With β-actin as the internal reference, the relative gene expression was calculated by $2^{-\Delta\Delta CT}$. The specific primer sequences are listed in **Table 1**.

Evaluation of effects of PF on NF-κB p65 and p-NF-κB p65 protein expressions in colon tissues of rats with IBS by Western blotting

After modeling and administration, the colon tissues were harvested, lysed and centrifuged, and the supernatant was collected to measure the total protein concentration. After

Table 1. Primer sequences

Gene	Primer sequence (5′-3′)
TNF-α	Forward: GAGCACGGAAAGCATGATCC
	Reverse: TAGACAGAAGAGCGTGGTGG
IL-1β	Forward: GGGATGATGACGACCTGCTA
	Reverse: TGTCGTTGCTTGTCTCTCCT
TGF-β	Forward: CTCATTCTGTCTCGAGCCCA
	Reverse: TGAAGTAGGGAAGGCAGTGG
ZO-1	Forward: TATCCAAACCAGACCCACCC
	Reverse: GGCTTTGGTGTGAATCGGTT
Occludin	Forward: TCCAACGGCAAAGTGAATGG
	Reverse: ACCTGTCGTGTAGTCGGTTT
β-actin	Forward: TCTTCCAGCCTTCCTTCCTG
	Reverse: CACACAGAGTACTTGCGCTC

TNF-α, tumor necrosis factor-α; IL-1β, interleukin-1β; TGF-β, transforming growth factor-β; ZO-1, zonula occludens-1.

https://doi.org/10.4142/jvs.22083

denaturation, 30 μg of protein samples were taken, subjected to electrophoresis and transferred onto a membrane. Then the membrane was blocked and incubated with primary antibodies against NF-κB p65 (1:1,000) and p-NF-κB p65 (1:1,000) at 4°C overnight and then with secondary antibodies at room temperature for 2 h, followed by washing, color development and imaging. The gray value of band was analyzed by ImageJ.

Evaluation of effects of PF on intestinal flora of rats with IBS by 16S rRNA high-throughput sequencing

Since high-dose PF exerted the best efficacy, 6 samples were selected for 16S rRNA high-throughput sequencing each from normal, model and high-dose PF groups. The changes in intestinal flora were observed.

Total genomic DNA was extracted from cecal contents by cetyltrimethylammonium bromide/sodium dodecyl sulfate, and its concentration and purity were detected by 1% agarose gel. Based on the concentration, DNA was diluted to 1 ng/μL with sterile water.

The V3-V4 region of 16S rRNA gene was amplified using primers 338F (5′-ACTCCTACGGGAGGCAGCAG-3′) and 806R (5′-GGACTACHVGGGTWTCTAAT-3′). The PCR amplification system consisted of 10 ng of template DNA, 0.2 μM of forward primers, 0.2 μM of reverse primers, and 15 μL of Phusion High-Fidelity PCR Master Mix (New England Biolabs, UK). The reaction conditions were as follows: pre-denaturation at 98°C for 1 min, then 15 cycles of denaturation at 95°C for 10 sec, annealing at 50°C for 30 sec, and extension at 72°C for 30 sec, insulation at 72°C for 5 min and storage at 4°C. The PCR products were purified and mixed using Qiagen Gel Extraction Kit (Qiagen, Germany), followed by 2% agarose gel electrophoresis. Sequencing libraries were generated using TruSeq DNA PCR-Free Sample Preparation Kit (Illumina, USA), and its quality was assessed by Qubit 2.0 Fluorometer (Thermo Scientific) and 2100 Bioanalyzer system (Agilent, USA). Finally, library sequencing was conducted by NovaSeq (Illumina), generating 250 bp paired-end sequences.

After assembly and quality control of raw sequencing data using FLASH V1.2.7 (Center for Bioinformatics and Computational Biology, USA; http://ccb.jhu.edu/software/FLASH/), the effective Tags were finally obtained. At the 97% similarity level, the Tags were clustered using Uparse software, v7.0.1001 (Uparse, USA; http://drive5.com/uparse/) into operational taxonomic units (OTUs). Then the taxonomic information of OTUs was labeled by Silva database (http://www.arb-silva.de/) based on the Mothur algorithm, and MUSCLE software, version 3.8.31 (Robert Edgar, UK; http://www.drive5.com/muscle/) was used for multiple sequence alignment. The OTU abundance information was normalized using a standard of sequence number corresponding to the sample with the least sequences. Then α- and β-diversity analyses were performed. The intergroup difference in diversity index was detected through the Wilcoxon rank-sum test, differential bacteria were screened by the Kruskal-Wallis rank-sum test (Games-Howell *post hoc* test) combined with false discovery rate multiple test, and $p < 0.05$ was considered statistically significant. Finally, the related gene pathways that may be affected by differential bacteria were predicted by the Phylogenetic Investigation of Communities by Reconstruction of Unobserved States database.

Statistical analysis

SPSS 20.0 software (IBM, USA) was used for statistical analysis. Measurement data were expressed as ($\bar{x} \pm s$). Multigroup comparisons were conducted by one-way analysis of variance,

https://doi.org/10.4142/jvs.22083

and pairwise comparisons were carried out with the Bonferroni test. The p values < 0.05 was considered statistically significant.

RESULTS

Visceral sensitivity

The AWR score at 20 mmHg pressure and pain threshold had significant differences between normal and model groups ($p < 0.01$). Compared with the model group, positive drug and PF groups had significantly decreased AWR scores at 20 mmHg pressure and increased pain threshold ($p < 0.05$, $p < 0.01$). The AWR score at above 20 mmHg pressure significantly rose in each group, without significant differences ($p > 0.05$) (**Table 2**).

Fecal water contents

After modeling and administration, the fecal water content significantly rose in the model group compared with that of the normal group ($p < 0.01$), while it decreased in positive drug and PF groups compared with that of the model group ($p < 0.05$, $p < 0.01$) (**Fig. 2A**).

HE staining results

It was observed by HE staining that in the normal group, the colon tissue had an intact structure, the colonic mucosa was normal in morphology, the mucosal epithelium was intact and continuous in a simple columnar shape, the glands were regularly arranged and clear in structure, and the muscularis mucosa was discerned in the lamina propria. In the model group, the mucosal layer of colon tissues was discontinuous, the glands were arranged disorderly with unclear boundaries, and the lamina propria almost had no visible muscularis mucosa but had obvious inflammatory cell infiltration. In positive drug and PF groups, the pathological morphology of colon tissues was greatly improved, the mucosal morphology was relatively intact, the glands were arranged neatly and clear in structure, and no obvious inflammatory cell infiltration was found (**Fig. 2B**).

Serum D-lactate levels

After modeling and administration, the level of serum D-lactate in the model group was significantly higher than that of the normal group ($p < 0.01$), while it was lower in positive drug and PF groups than that of the model group ($p < 0.05$, $p < 0.01$) (**Fig. 3A**).

Inflammatory factors

The model group had significantly increased levels of serum IL-1β, TGF-β, and TNF-α compared with those of the normal group, while positive drug and PF groups had significantly decreased levels compared with those of the model group ($p < 0.05$, $p < 0.01$) (**Fig. 3B**).

Table 2. AWR score and pain threshold after modeling and administration

Group	AWR score (20 mmHg)	AWR score (40 mmHg)	AWR score (60 mmHg)	AWR score (80 mmHg)	Pain threshold (mmHg)
Control	1.03 ± 0.60	2.27 ± 0.61	3.60 ± 0.33	3.77 ± 0.42	47.42 ± 7.07
Model	2.13 ± 0.56[a]	3.20 ± 0.67[a]	3.80 ± 0.27	3.97 ± 0.10	29.50 ± 7.83[a]
Positive control	1.33 ± 0.54[c]	2.63 ± 0.41[b]	3.77 ± 0.21	3.83 ± 0.27	41.57 ± 7.40[c]
PF-low dose	1.60 ± 0.49[b]	3.23 ± 0.6	3.80 ± 0.16	3.97 ± 0.10	30.10 ± 8.06
PF-middle dose	1.43 ± 0.40[c]	2.80 ± 0.54	3.70 ± 0.23	3.93 ± 0.20	36.67 ± 6.38[b]
PF-high dose	1.40 ± 0.42[c]	2.80 ± 0.49[b]	3.67 ± 0.26	3.87 ± 0.31	38.33 ± 4.68[c]

Normal group, model group, positive drug group, low-dose PF group, medium-dose PF group and high-dose PF group (n = 10).
AWR, abdominal withdrawal reflex; PF, paeoniflorin.
[a]$p < 0.01$ vs. normal group, [b]$p < 0.05$ vs. model group, [c]$p < 0.01$ vs. model group.

https://doi.org/10.4142/jvs.22083

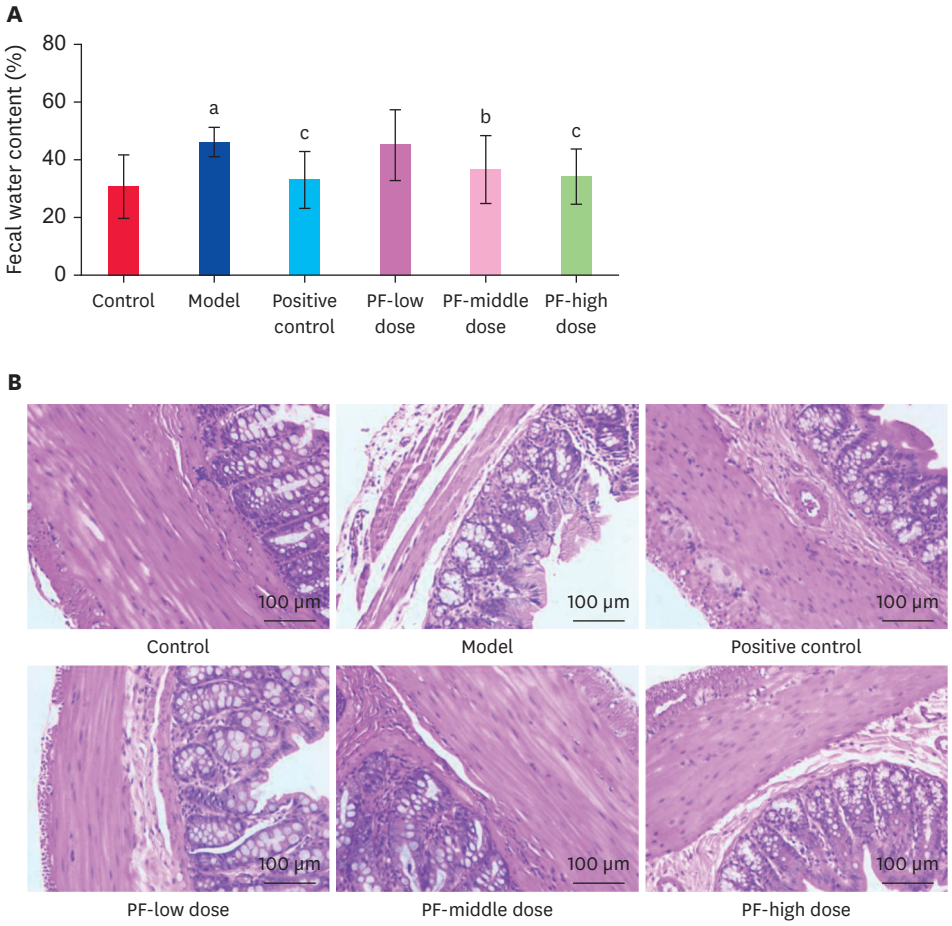

Fig. 2. Fecal water contents. (A) Fecal water contents after modeling and administration. (B) HE staining results of colon tissues (200×). Normal group, model group, positive drug group, low-dose PF group, medium-dose PF group and high-dose PF group (n = 10).
HE, hematoxylin-eosin; PF, paeoniflorin.
[a]$p < 0.01$ vs. normal group, [b]$p < 0.05$ vs. model group, [c]$p < 0.01$ vs. model group.

The mRNA levels of IL-1β, TGF-β, and TNF-α in the model group were significantly higher than those of the normal group ($p < 0.01$), while they were significantly lower in positive drug and PF groups than those of the model group ($p < 0.05$, $p < 0.01$) (**Fig. 3C**).

Changes in p-NF-κB p65 protein expression

There was a significantly higher protein expression of p-NF-κB p65 in the model group than in the normal group ($p < 0.01$), while the protein expression of p-NF-κB p65 significantly reduced in positive drug and PF groups compared with that of the model group ($p < 0.05$, $p < 0.01$) (**Fig. 3D**).

Changes in intestinal permeability

Compared with the normal group, the model group had significantly decreased mRNA levels of ZO-1 and occludin ($p < 0.01$). Compared with the model group, positive drug and PF groups had significantly increased mRNA levels of ZO-1 and occludin ($p < 0.05$, $p < 0.01$) (**Fig. 4A**).

The ZO-1 and occludin positive expression area became significantly smaller in the model group than that in the normal group ($p < 0.01$), but it became significantly larger in positive drug and PF groups than that in the model group ($p < 0.05$, $p < 0.01$) (**Fig. 4B and C**).

https://doi.org/10.4142/jvs.22083

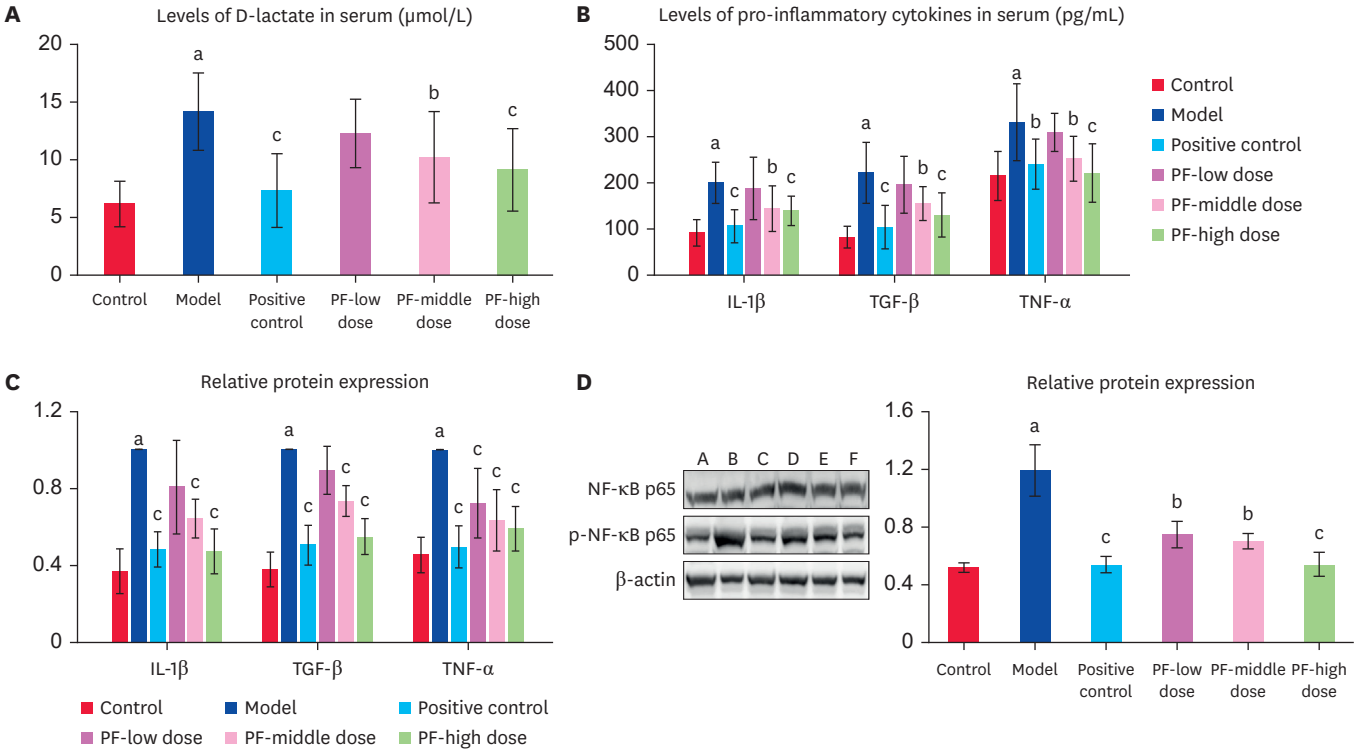

Fig. 3. Levels of serum D-lactate and inflammatory factors. (A) Serum D-lactate levels. Normal group, model group, positive drug group, low-dose PF group, medium-dose PF group and high-dose PF group (n = 10). (B) Levels of serum pro-inflammatory factors. Normal group, model group, positive drug group, low-dose PF group, medium-dose PF group and high-dose PF group (n = 10). (C) mRNA levels of inflammatory factors in colon tissues. Normal group, model group, positive drug group, low-dose PF group, medium-dose PF group and high-dose PF group (n = 6). (D) Protein levels of inflammatory factors in colon tissues. Normal group, model group, positive drug group, low-dose PF group, medium-dose PF group and high-dose PF group (n = 3).
PF, paeoniflorin; mRNA, messenger RNA; IL-1β, interleukin-1β; TGF-β, transforming growth factor-β; TNF-α, tumor necrosis factor-α.
[a]$p < 0.01$ vs. control group, [b]$p < 0.05$ vs. model group, [c]$p < 0.01$ vs. model group.

Effect of PF on intestinal flora

To explore the effect of high-dose PF on the intestinal flora of model rats, 16S rRNA high-throughput sequencing was conducted for the fecal flora. A total of 1,180 OTUs were obtained from 18 samples, and the abundance and diversity of intestinal flora were determined by α-diversity analysis (Shannon index). The Shannon index of the model group was higher than that of the normal group ($p < 0.05$), while it was lower in PF groups than that in the model group ($p < 0.05$), suggesting that the intestinal flora changed in normal, model and PF groups (**Fig. 5A**).

Then the composition of intestinal flora in different samples was determined through β-diversity analysis, and assessed by principal coordinate analysis (PCoA) based on the binary_Jaccard distance. The linear distance was smaller at a higher similarity of composition among samples. On the contrary, the linear distance was larger at a lower similarity among samples (**Fig. 5B**). The results of PCoA showed that the sample points were completely separated in normal, model and PF groups. Similar results were obtained in cluster analysis. The above findings suggest that the overall structure and composition of intestinal flora varied greatly after PF administration (**Fig. 5C**).

To further explore the α- and β-diversities in the composition of intestinal flora, the number of shared and unique OTUs in different groups was analyzed through Venn diagram to

https://doi.org/10.4142/jvs.22083

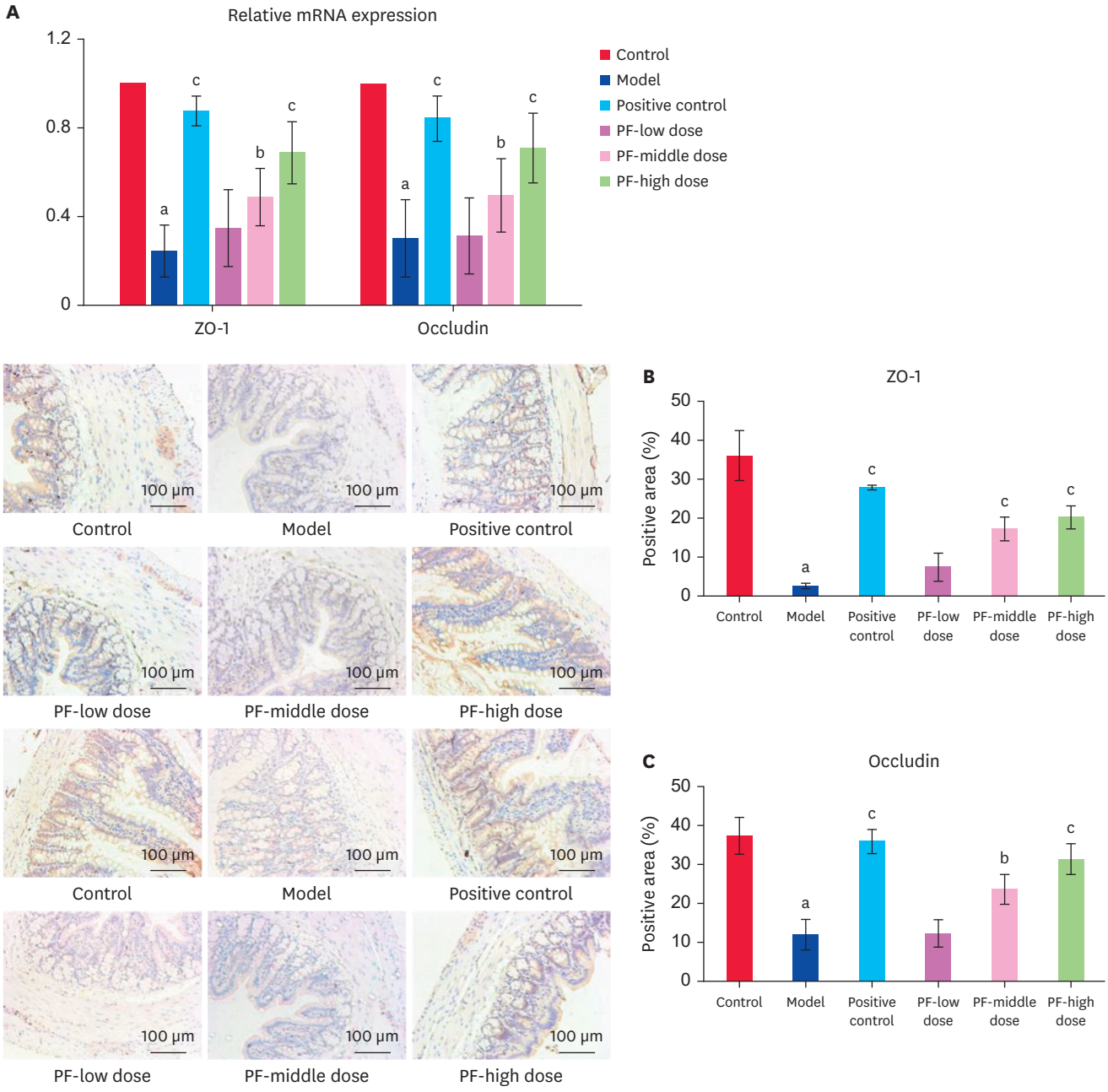

Fig. 4. Changes in intestinal permeability. (A) mRNA levels of ZO-1 and occludin in colon tissues (n = 6). (B) ZO-1 level in colon tissues (n = 6). (C) Occludin level in colon tissues (n = 6).
mRNA, messenger RNA; ZO-1, zonula occludens-1; PF, paeoniflorin.
[a]$p < 0.01$ vs. control group, [b]$p < 0.05$ vs. model group, [c]$p < 0.01$ vs. model group.

intuitively display the similarity and overlapping of OTUs among samples. It was found that the number of shared OTUs was 456 among normal, model and PF groups (**Fig. 6A**).

The composition of intestinal flora at the phylum level is exhibited in **Fig. 6B**. Firmicutes and Bacteroidetes were dominant bacteria, and the Firmicutes/Bacteroidetes ratio significantly rose in the model group compared with that of the normal group ($p < 0.01$), while it significantly decreased in PF groups compared with that in the model group ($p < 0.01$) (**Fig. 6C**). At the

https://doi.org/10.4142/jvs.22083

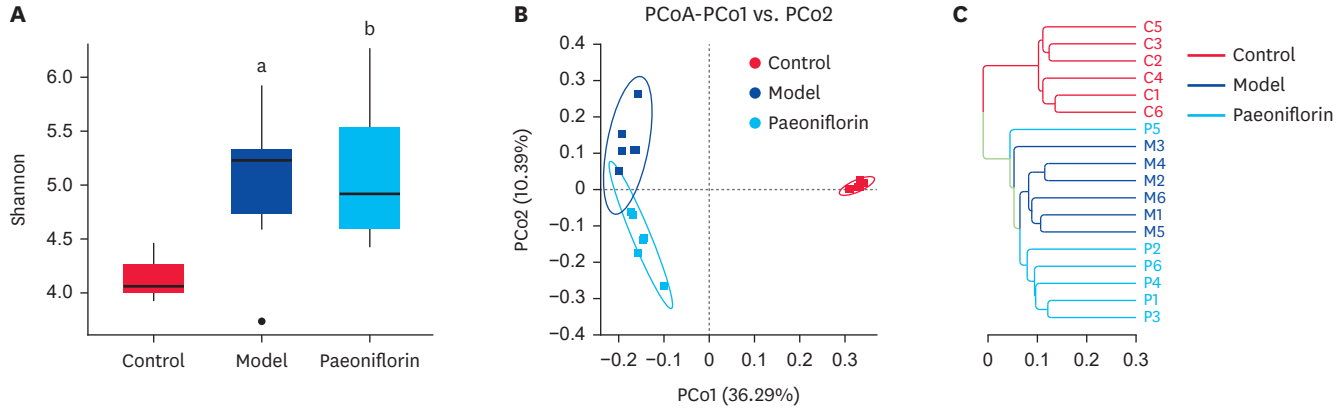

Fig. 5. 16S rRNA high-throughput sequencing for the fecal flora and composition of intestinal flora in different samples. (A) Shannon index (n = 6). (B) PCoA diagram (n = 6). (C) Cluster analysis results (n = 6).
PCoA, principal coordinate analysis.
[a]$p < 0.05$ vs. control group, [b]$p < 0.05$ vs. model group.

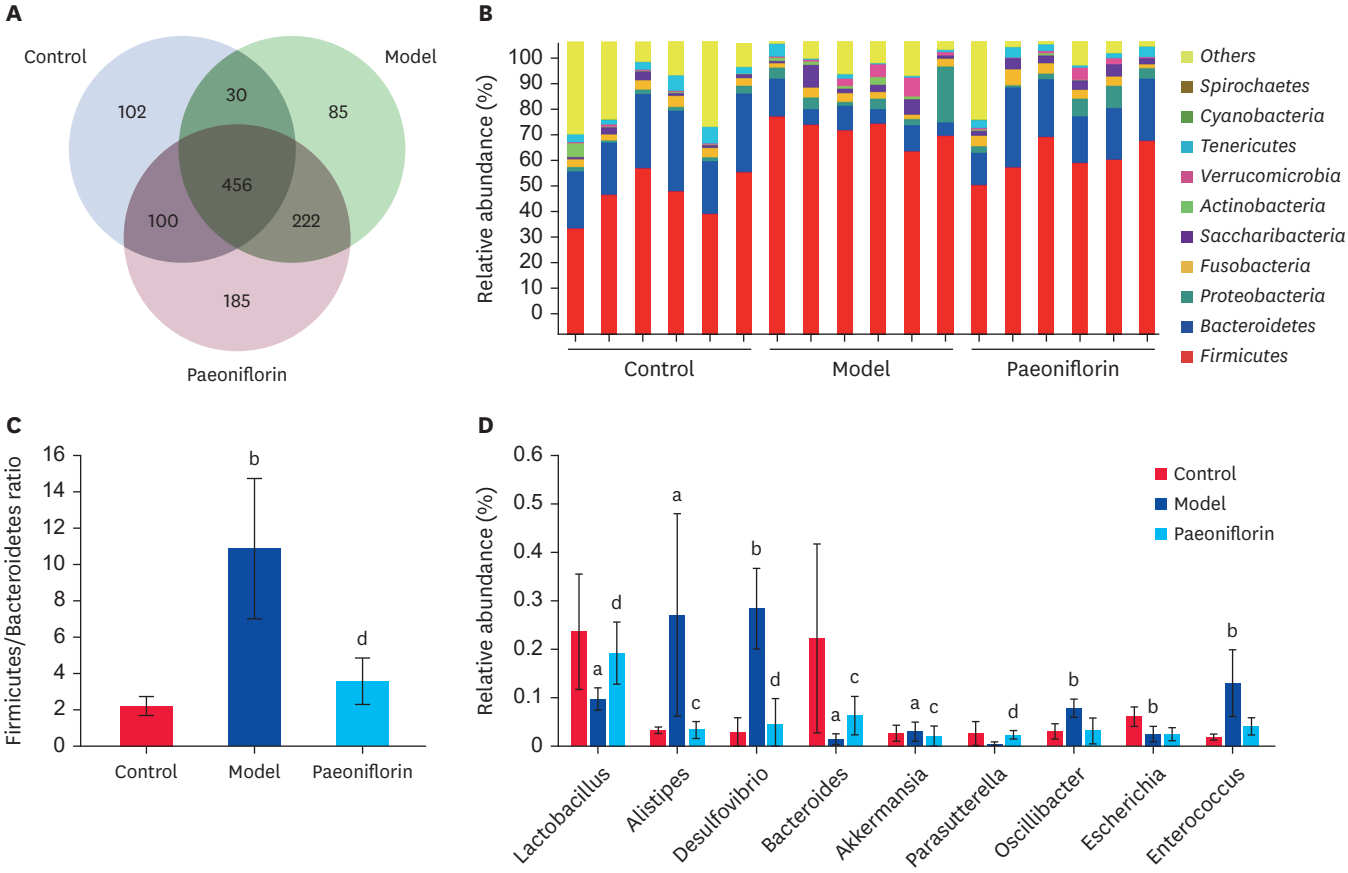

Fig. 6. α- and β-diversities in the composition of intestinal flora and composition of intestinal flora at the phylum level. (A) Venn diagram (n=6). (B) Intestinal flora at the phylum level (n = 6). (C) Firmicutes/Bacteroidetes ratio (n = 6). (D) Intestinal flora at the genus level (n = 6).
[a]$p < 0.05$ vs. control group, [b]$p < 0.01$ vs. control group, [c]$p < 0.05$ vs. model group, [d]$p < 0.01$ vs. model group.

genus level, the abundance of *Lactobacillus*, *Alistipes*, *Akkermansia*, *Bacteroides*, and *Oscillibacter* was lower, while the abundance of *Desulfovibrio*, *Escherichia*, and *Enterococcus* was higher in the model group than those in the normal group. PF groups had higher abundance of

https://doi.org/10.4142/jvs.22083

Lactobacillus, *Akkermansia*, *Alistipes*, and *Bacteroides*, but lower abundance of *Desulfovibrio*, *Parasutterella*, and *Enterococcus* than those of the model group (**Fig. 6D**).

DISCUSSION

PF is one of the main active ingredients of *Paeonia lactiflora* and a monoterpenoid glycoside compound. It can greatly mitigate the pain caused by warm bathing and bee venom in mice, alleviate colitis in mice, and resist adjuvant arthritis in rats. Additionally, it can protect the nerve, blood-brain barrier, local cerebral blood flow and endothelial cells, prevent cerebral edema after cerebral ischemia, ameliorate scopolamine-induced spatial learning memory dysfunction, and block L-type calcium channel in rat cardiomyocytes [12,13]. However, the therapeutic effect of PF on IBS has not been reported yet.

The pathogenesis of IBS has been associated with gastrointestinal mobility disorders, visceral hypersensitivity, chronic intestinal inflammation, alteration of intestinal flora and psychological problems [14,15]. Visceral hypersensitivity means the viscera suffer from discomfort or pain due to physiological stimuli and have strong response to noxious stimuli, reducing the pain tolerance threshold [16]. One of the most prevalent symptoms of IBS is spontaneous abdominal pain, and long-term pain can be physically and mentally draining. In this study, the AWR score at 20 mmHg pressure and pain threshold had significant differences between normal and model groups. Compared with the model group, positive drug and PF groups had significantly decreased AWR scores at 20 mmHg pressure and increased pain threshold. Tight junction proteins, such as ZO-1 and occludin, are important proteins involved in the formation of intestinal mucosal mechanical barrier [17], which regulate and maintain the intestinal permeability and cell polarity. As a result, the intestinal tract selectively absorbs nutrients and water, and blocks the invasion of pathogens such as bacteria and viruses. When the amount of oxidants exceeds that of antioxidants, oxidative stress occurs, causing an imbalance between oxidation and antioxidation. Then tissues are damaged and tissue structures are destroyed, resulting in inflammation [18]. Herein, compared with the normal group, the colon tissues and cells were arranged loosely and disorderly, the morphology of mucosal epithelium was changed, there was a small amount of inflammatory cell infiltration, the levels of IL-1β, TGF-β, TNF-α, D-lactate, and p-NF-κB p65 protein and the fecal water content significantly rose, and the levels of ZO-1 and occludin declined in model and PF groups. Compared with the model group, the colon tissues and cells were arranged tightly, the morphology of mucosal epithelium was intact, there was mild inflammatory cell infiltration, the levels of IL-1β, TGF-β, TNF-α, D-lactate, and p-NF-κB p65 protein and the fecal water content declined, and the levels of ZO-1 and occludin rose in PF groups. Taken together, PF can ameliorate oxidative stress, raise the expressions of ZO-1 and occludin, and regulate the intestinal permeability, thereby protecting the intestinal tract.

The gastrointestinal tract of healthy adults harbors a variety of diverse microorganisms, collectively known as the intestinal flora. About 10^{14} microorganisms colonize the digestive tract of healthy adults, far more than the total number of human cells, and the number of intestinal bacterial species detected based on high-throughput sequencing exceeds 1,000 [19,20]. As a complex and active micro-ecosystem, the normal intestinal flora is closely related to human health and jointly implicated in host physiological processes such as nutrient absorption, metabolism, growth and development, and immunoregulation. Due to various internal and external factors, such as the environment, diet and emotions, the human

intestinal micro-ecosystem changes, thus inducing diseases inside and outside the intestine [21]. The stability of intestinal flora in IBS patients is lower than that of healthy individuals, so the patients have poorer intestinal function. In IBS patients, the relative abundances of some Firmicutes bacteria (e.g., *Ruminococcaceae* spp. and *Clostridium* cluster XIVa) increase, but those of some bacteria decrease. Nevertheless, the intestinal flora is diverse and complex, so the bacteria that have been verified to be related with IBS remain limited [22,23]. α-Diversity analysis is mainly used to reflect the diversity of intestinal flora, which can be assessed by Shannon and Simpson indexes [24]. The Simpson index of IBS model rats is lower than that of normal rats [25]. Besides, the Shannon index of IBS group is 1.2 times lower than that of healthy group ($p = 0.008$) [26]. It is well-documented that PF has obvious therapeutic effects on animals with ulcerative colitis, which has mainly been attributed to anti-inflammatory and immune-regulatory roles [27,28]. However, due to low permeability and efflux by P-glycoprotein, PF cannot be easily absorbed, with the oral bioavailability of only 3%–4%, and the level in rat feces is much higher than that in the plasma [29]. Hence, PF works primarily in the intestinal tract. IBS patients have decreased biodiversity and stability, and the reduction in bacterial diversity results in the loss or decrease of important functions that maintain the gut barrier integrity and regulate the host immune system. In the meantime, mucolytic and pathogenic bacteria also increase, giving a compromised mucosal barrier and allowing more pathogens to invade the intestinal tissue [30].

In this study, to explore the effect of high-dose PF on the intestinal flora of model rats, 16S rRNA high-throughput sequencing was conducted for the fecal flora. A total of 1,180 OTUs were obtained from 18 samples. The Shannon index of the model group was higher than that of the normal group ($p < 0.05$), while it was lower in PF groups than that of the model group ($p < 0.05$), suggesting that there were changes in the intestinal flora of normal, model and PF groups. Then the composition of intestinal flora in different samples was explored through β-diversity analysis, and assessed by PCoA. The results showed that the sample points were completely separated in normal, model and PF groups. Similar results were also obtained in cluster analysis. Collectively, the overall structure and composition of intestinal flora varied greatly after PF administration. To further explore the α- and β-diversity in the composition of intestinal flora, the number of shared and unique OTUs in different groups was determined through Venn diagram to intuitively display the similarity and overlapping of OTUs among samples. It was found that the number of shared OTUs was 456 among normal, model and PF groups.

The intestinal mucosal biological barrier is mainly composed of commensal bacteria colonized on the surface. These bacteria can inhibit the growth of exogenous pathogenic bacteria by producing bacteriostatic substances or nutrient competition. When the intestinal flora is imbalanced, the function of the barrier is destroyed, further damaging the mechanical and immune barriers [31]. *Lactobacillus* inhibits the colonization of pathogens in the intestinal tract and relieves the harm of colonic inflammation [32]. Meanwhile, the bacteria can promote the production of short chain fatty acids and growth [33]. *Akkermansia* accounts for 1%–5% of the human gut microbiome [34], with the largest colonization on the cecum [35]. *Akkermansia* is a Gram-negative anaerobic bacterium that degrades mucin as the sole carbon source, and also stimulates mucin production to alter the thickness of the mucus layer, playing a key role in the mucosal interface between the lumen and epithelial cells [36]. Given that the colonization level of *Akkermansia* in the intestinal mucosa of IBD patients is significantly lower than that of healthy people [37], *Akkermansia* is implicated in the onset and progression of IBD.

At the phylum level, Firmicutes and Bacteroidetes were dominant bacteria, and the Firmicutes/Bacteroidetes ratio significantly rose in the model group compared with that of the normal group, while it significantly declined in PF groups compared with that of the model group. At the genus level, the abundance of *Lactobacillus*, *Alistipes*, *Akkermansia*, *Bacteroides*, and *Oscillibacter* was lower, while the abundance of *Desulfovibrio*, *Escherichia*, and *Enterococcus* was higher in the model group than those of the normal group. PF groups had higher abundance of *Lactobacillus*, *Akkermansia*, *Alistipes*, and *Bacteroides*, but lower abundance of *Desulfovibrio*, *Parasutterella*, and *Enterococcus* than those of the model group.

In conclusion, PF can up-regulate the abundance of *Lactobacillus*, *Akkermansia*, *Alistipes* and *Bacteroides*, down-regulate the abundance of *Desulfovibrio*, *Parasutterella*, and *Enterococcus*, raise the expressions of ZO-1 and occludin in colon tissues, and reduce the levels of IL-1β, TGF-β, TNF-α, D-lactate, and p-NF-κB p65 in IBS model rats, thereby exerting a therapeutic effect on IBS. Regardless, this study is limited. The findings have been proven only in a rat model, but the dose-effect relationship, pharmacodynamic effect and mechanism need to be further explored. In the future, the therapeutic effects of PF on IBS need to be further verified by performing double-blind randomized controlled trials.

REFERENCES

1. Wilson B, Rossi M, Kanno T, Parkes GC, Anderson S, Mason AJ, et al. β-Galactooligosaccharide in conjunction with low FODMAP diet improves irritable bowel syndrome symptoms but reduces fecal bifidobacteria. Am J Gastroenterol. 2020;115(6):906-915.
PUBMED | CROSSREF
2. Liu Y, Xiao W, Yu L, Tian F, Wang G, Lu W, et al. Evidence from comparative genomic analyses indicating that *Lactobacillus*-mediated irritable bowel syndrome alleviation is mediated by conjugated linoleic acid synthesis. Food Funct. 2021;12(3):1121-1134.
PUBMED | CROSSREF
3. Chang KM, Lee MH, Lin HH, Wu SL, Wu HC. Does irritable bowel syndrome increase the risk of interstitial cystitis/bladder pain syndrome? A cohort study of long term follow-up. Int Urogynecol J Pelvic Floor Dysfunct. 2021;32(5):1307-1312.
PUBMED | CROSSREF
4. Ma Q, Ouyang Y, Meng F, Noolvi MN, Avvaru SP, More UA, et al. A review of pharmacological and clinical studies on the application of Shenling Baizhu San in treatment of ulcerative colitis. J Ethnopharmacol. 2019;244:112105.
PUBMED | CROSSREF
5. Bao CH, Wang CY, Li GN, Yan YL, Wang D, Jin XM, et al. Effect of mild moxibustion on intestinal microbiota and NLRP6 inflammasome signaling in rats with post-inflammatory irritable bowel syndrome. World J Gastroenterol. 2019;25(32):4696-4714.
PUBMED | CROSSREF
6. Hou JJ, Wang X, Li Y, Su S, Wang YM, Wang BM. The relationship between gut microbiota and proteolytic activity in irritable bowel syndrome. Microb Pathog. 2021;157:104995.
PUBMED | CROSSREF
7. Wang YH, Li B, Cai GX, Yang H. Comparative study on effect of three preparations of Xiaoyao formula on soothing liver and strengthening spleen. Zhongguo Zhongyao Zazhi. 2012;37(19):2951-2955.
PUBMED
8. Li C, Ding L, Ding F, Hu S, Wang L, Chen J. Influence of ingredient combination and peoniflorin content on the blood-nourishing,liver-soothing and pain-relieving actions of Radix Paeoniae Alba. Zhongyao Xinyao Yu Linchuang Yaoli. 2011;22(1):54-56.
9. Yu HY, Liu MG, Liu DN, Shang GW, Wang Y, Qi C, et al. Antinociceptive effects of systemic paeoniflorin on bee venom-induced various 'phenotypes' of nociception and hypersensitivity. Pharmacol Biochem Behav. 2007;88(2):131-140.
PUBMED | CROSSREF

10. Sun H, Li X, Chen W, Jia F, Su J, Zhang B, et al. Effect of probiotics and dietary fiber combined with pinaverium bromide on intestinal flora in patients with irritable bowel syndrome. Am J Transl Res. 2021;13(12):14039-14045.
PUBMED

11. Hong KB, Seo H, Lee JS, Park Y. Effects of probiotic supplementation on post-infectious irritable bowel syndrome in rodent model. BMC Complement Altern Med. 2019;19(1):195.
PUBMED | CROSSREF

12. Tabata K, Matsumoto K, Watanabe H. Paeoniflorin, a major constituent of peony root, reverses muscarinic M1-receptor antagonist-induced suppression of long-term potentiation in the rat hippocampal slice. Jpn J Pharmacol. 2000;83(1):25-30.
PUBMED | CROSSREF

13. Zhang D, Chang S, Li X, Shi H, Jing B, Chen Z, et al. Therapeutic effect of paeoniflorin on chronic constriction injury of the sciatic nerve via the inhibition of Schwann cell apoptosis. Phytother Res. 2022;36(6):2572-2582.
PUBMED | CROSSREF

14. Pittayanon R, Lau JT, Yuan Y, Leontiadis GI, Tse F, Surette M, et al. Gut microbiota in patients with irritable bowel syndrome-a systematic review. Gastroenterology. 2019;157(1):97-108.
PUBMED | CROSSREF

15. Ansari F, Pourjafar H, Tabrizi A, Homayouni A. The effects of probiotics and prebiotics on mental disorders: a review on depression, anxiety, Alzheimer, and autism spectrum disorders. Curr Pharm Biotechnol. 2020;21(7):555-565.
PUBMED | CROSSREF

16. Kamphuis JB, Guiard B, Leveque M, Olier M, Jouanin I, Yvon S, et al. Lactose and fructo-oligosaccharides increase visceral sensitivity in mice via glycation processes, increasing mast cell density in colonic mucosa. Gastroenterology. 2020;158(3):652-663.e6.
PUBMED | CROSSREF

17. Chen L, Li L, Han Y, Lv B, Zou S, Yu Q. Tong-Fu-Li-Fei decoction exerts a protective effect on intestinal barrier of sepsis in rats through upregulating ZO-1/occludin/claudin-1 expression. J Pharmacol Sci. 2020;143(2):89-96.
PUBMED | CROSSREF

18. Li Z, Chang L, Ren X, Hu Y, Chen Z. Modulation of rat kidney stone crystallization and the relative oxidative stress pathway by green tea polyphenol. ACS Omega. 2021;6(2):1725-1731.
PUBMED | CROSSREF

19. Ji HJ, Kang N, Chen T, Lv L, Ma XX, Wang FY, et al. Shen-Ling-Bai-Zhu-San, a spleen-tonifying Chinese herbal formula, alleviates lactose-induced chronic diarrhea in rats. J Ethnopharmacol. 2019;231:355-362.
PUBMED | CROSSREF

20. Benítez-Páez A, Hartstra AV, Nieuwdorp M, Sanz Y. Gut microbiota survey at species-and strain-level using long-amplicon sequencing, and its application to trace species engraftment. bioRxiv. 2021 Oct 27. https://doi.org/10.1101/2020.09.11.292896.

21. Dannenberg L, Zikeli D, Benkhoff M, Ahlbrecht S, Kelm M, Levkau B, et al. Targeting the human microbiome and its metabolite TMAO in cardiovascular prevention and therapy. Pharmacol Ther. 2020;213:107584.
PUBMED | CROSSREF

22. Jeffery IB, O'Toole PW, Öhman L, Claesson MJ, Deane J, Quigley EM, et al. An irritable bowel syndrome subtype defined by species-specific alterations in faecal microbiota. Gut. 2012;61(7):997-1006.
PUBMED | CROSSREF

23. Rajilić-Stojanović M, Biagi E, Heilig HG, Kajander K, Kekkonen RA, Tims S, et al. Global and deep molecular analysis of microbiota signatures in fecal samples from patients with irritable bowel syndrome. Gastroenterology. 2011;141(5):1792-1801.
PUBMED | CROSSREF

24. Zhu HM, Li L, Li SY, Yan Q, Li F. Effect of water extract from Berberis heteropoda Schrenk roots on diarrhea-predominant irritable bowel syndrome by adjusting intestinal flora. J Ethnopharmacol. 2019;237:182-191.
PUBMED | CROSSREF

25. Wang X, Qi Q, Wang Y, Wu H, Jin X, Yao H, et al. Gut microbiota was modulated by moxibustion stimulation in rats with irritable bowel syndrome. Chin Med. 2018;13(1):63.
PUBMED | CROSSREF

26. Carroll IM, Ringel-Kulka T, Keku TO, Chang YH, Packey CD, Sartor RB, et al. Molecular analysis of the luminal- and mucosal-associated intestinal microbiota in diarrhea-predominant irritable bowel syndrome. Am J Physiol Gastrointest Liver Physiol. 2011;301(5):G799-G807.
PUBMED | CROSSREF

27. Xu JH, Ao H, Hong JQ, Zhou JY, Weng YJ, Zhang JD, et al. Paeoniflorin inhibits lipopolysaccharide-induced microglia inflammation and phagocytosis through IL-10-STAT3 signaling pathway. Chin J Biochem Mol Biol. 2017;33:169-175.
28. Liu J, Zhao Z, Wei Y, Xu F, Zhang H, Li M, et al. Inhibitory effect of paeoniflorin on inflammatory chemokines and their receptor in a mouse model of asthma. Acta Lab Anim Sci Sin. 2016;24:460-464.
29. Zhou YX, Gong XH, Zhang H, Peng C. A review on the pharmacokinetics of paeoniflorin and its anti-inflammatory and immunomodulatory effects. Biomed Pharmacother. 2020;130:110505.
PUBMED | CROSSREF
30. Sheehan D, Moran C, Shanahan F. The microbiota in inflammatory bowel disease. J Gastroenterol. 2015;50(5):495-507.
PUBMED | CROSSREF
31. Wu XX, Huang XL, Chen RR, Li T, Ye HJ, Xie W, et al. Paeoniflorin prevents intestinal barrier disruption and inhibits lipopolysaccharide (LPS)-induced inflammation in Caco-2 cell monolayers. Inflammation. 2019;42(6):2215-2225.
PUBMED | CROSSREF
32. Egerton S, Donoso F, Fitzgerald P, Gite S, Fouhy F, Whooley J, et al. Investigating the potential of fish oil as a nutraceutical in an animal model of early life stress. Nutr Neurosci. 2022;25(2):356-378.
PUBMED | CROSSREF
33. Lemaire M, Dou S, Cahu A, Formal M, Le Normand L, Romé V, et al. Addition of dairy lipids and probiotic Lactobacillus fermentum in infant formula programs gut microbiota and entero-insular axis in adult minipigs. Sci Rep. 2018;8(1):11656.
PUBMED | CROSSREF
34. Derrien M, Collado MC, Ben-Amor K, Salminen S, de Vos WM. The mucin degrader *Akkermansia muciniphila* is an abundant resident of the human intestinal tract. Appl Environ Microbiol. 2008;74(5):1646-1648.
PUBMED | CROSSREF
35. Derrien M, Van Baarlen P, Hooiveld G, Norin E, Müller M, de Vos WM. Modulation of mucosal immune response, tolerance, and proliferation in mice colonized by the mucin-degrader *Akkermansia muciniphila*. Front Microbiol. 2011;2:166.
PUBMED | CROSSREF
36. Schroeder BO. Fight them or feed them: how the intestinal mucus layer manages the gut microbiota. Gastroenterol Rep (Oxf). 2019;7(1):3-12.
PUBMED | CROSSREF
37. Png CW, Lindén SK, Gilshenan KS, Zoetendal EG, McSweeney CS, Sly LI, et al. Mucolytic bacteria with increased prevalence in IBD mucosa augment *in vitro* utilization of mucin by other bacteria. Am J Gastroenterol. 2010;105(11):2420-2428.
PUBMED | CROSSREF